Journal of Siberian Federal University. Engineering & Technologies 1 (2013 6) 15-27
~ ~ ~

УДК 532.5

Micro-LIF and Numerical Investigation of Mixing in Microchannel

Andrey V. Minakov[a,b]*, Anna A. Yagodnitsyna[b], Alexander S. Lobasov[a,b], Valery Ya. Rudyak[b,c] and Artur V. Bilsky[b]

[a] *Siberian Federal University, 28 Kirensky Str., Krasnoyarsk, 660074 Russia*

[b] *Institute of Thermophysics SB RAS, 1 Lavrentiev, Novosibirsk, 630090 Russia*

[c] *Novosibirsk State University of Civil Engineering, 113 Leningradskaya Str., 630008 Russia*

Received 11.02.2013, received in revised form 18.02.2013, accepted 25.02.2013

Flow regimes and mixing pattern in a T-type micromixer at high Reynolds numbers were studied by numerical solution of the Navier–Stokes equations and by particle image velocimetry (micro-PIV) and laser induced fluorescence (micro-LIF) experimental measurements. The Reynolds number was varied from 1 to 1000. The cross section of the mixing channel was 200 μm×400 μm, and its length was 3000 μm. Five different flow regimes were identified: (I) steady vortex-free flow; (II) steady symmetric vortex flow with two horseshoe vortices; (III) steady asymmetric vortex flow; (IV) unsteady periodic flow; (V) stochastic flow. Maximum mixing efficiency was obtained for stationary asymmetric vortex flow. In this case, an S-shaped vortex structure formed in the flow field. Good agreement between calculation and experiment was obtained.

Keywords: Microflow, Micromixers, Microchannels, CFD, Micro-PIV, Micro-LIF.

Introduction

Liquid mixing is an important physical process which is widely used in various microfluidic devices. Since the characteristic flow times are usually extremely small, mixing is accelerated using special devices called micromixers. Micromixers are a key element of many MEMS and other devices that are used in various biomedical and chemical technologies, creating different micro heat-exchangers, microapparatus, etc. The operating principles of micromixers and their optimization have been the subject of a great deal of research (see, for example, [1-4] and references therein). Most papers consider laminar flow at low Reynolds numbers, which are usually characteristic of microflow. In practice, however, there are situations when microflows Reynolds number (Re) are high enough [5,6]. In addition, at relatively high Reynolds numbers in microchannels take place number of new interesting phenomena requiring study both a fundamental point of view and for practical purposes.

* Corresponding author E-mail address: tov-andrey@yandex.ru

Thus, in the study of T-type micromixers the existence of critical Reynolds number at which the Dean vortices in a microchannel lost symmetry was experimentally demonstrated [1]. The critical Reynolds number about 150 for channel dimensions 600μm×300μm×300μm was found. Strong dependence of the critical Reynolds number from the channel size was shown. Transient flow regimes (at Reynolds number Re = 300-700) by the instrumentality of numerical simulation have been investigated in [7], but the mixing processes have not been studied. The mixing of two fluids in the range of Reynolds numbers from 50 to 1400 was studied experimentally and numerically in [8]. In [9] the existence of unsteady periodic regime for certain values of the Reynolds number first demonstrated numerically. The most comprehensive experimental study of mixing in a T-shaped microchannel at moderate Reynolds numbers (100-400) in [10] was carried out. There, using μ-LIF and μ-PIV measurements of the velocity and concentration fields in the various sections of the mixer was studied. For the first time the mixing efficiency was measured.

In spite of the relatively large number of papers covered the study of flow and mixing in T-type micromixers at moderate Reynolds numbers, in fact, sufficient systematic data about flow regimes and mixing processes took place in it is still absent. The present work covers systematic modeling of incompressible flow and mixing in a T-type micromixer at Reynolds numbers from 10 to 1000. The problem was solved numerically on the basis of the Navier-Stokes equations for an incompressible fluid. Verification of the simulation data was carried out experimentally. The measurements were performed by two methods: particle image velocimetry (micro-PIV) and laser induced fluorescence (micro-LIF).

Mathematical Model and Numerical Algorithm

The incompressible flows of multicomponent Newtonian fluids, which dynamics is described by the Navier-Stokes were considered

$$\frac{\partial \rho}{\partial t} + \nabla \cdot (\rho \mathbf{v}) = 0, \qquad \frac{\partial \rho \mathbf{v}}{\partial t} + \nabla \cdot (\rho \mathbf{v}\mathbf{v}) = -\nabla p + \nabla \cdot \hat{\mathbf{T}}, \tag{1}$$

where ρ is fluid density, p is pressure, $\mathbf{v}$ is its velocity, and $\hat{\mathbf{T}}$ is the viscous stress tensor. Density and viscosity of the mixture is determined by the mass fraction of mixture components f_i, the partial density ρ_i and molecular viscosity of the pure components μ_i

$$\rho = \sum_i f_i \rho_i \ , \ \mu = \sum_i f_i \cdot \mu_i \ ,$$

and the evolution of the mass concentrations determined by the equation

$$\frac{\partial \rho f_i}{\partial t} + \nabla \cdot (\rho f_i \mathbf{v}) = \nabla \cdot (\rho D_i \nabla f_i), \tag{2}$$

where D_i is the diffusion coefficient of the i-component.

As boundary conditions on the channel walls for the velocity vector components used slip or non-slip conditions. In this paper used the second one.

To solve the system of equations mentioned above CFD software package σFlow is used. A detailed description of the program numerical algorithm is given in [11,12]. The developed algorithm

used in solving a wide range of problems of external and internal flows [11-13]. Its applicability to describe the microflows shown in [14,15].

The investigation results of flow and mixing in T-type micromixers are presented in this paper. Width of the narrow channel part is 200 μm, width of the wide channel part is 400 μm, thickness of the channel is 200 μm and length of the mixing channel is 3000 μm. The problem is considered in the spatial and time-dependent formulation in the general case. Through the left channel input pure water is fed at a flow rate Q. Through the right channel input rhodamine-tinted water is fed at the same flow rate. The density of both fluids equals 1000 kg/m^3, the viscosity equals 0.001 Pa×s, the diffusion coefficient of the dye in water, $D = 2{,}63\times10^{-10}$ m^2/s. Thus, the value of Schmidt number for this problem is 3,800. As the boundary conditions at the entrance of the channel steady velocity profile was set. At the exit of the mixing channel Neumann conditions was set, i.e. vanishing of the normal to the output surface component of derivative of all scalar quantities.

The study was conducted for different values of Reynolds number, which is defined as follows: $\mathrm{Re} = (\rho U d/\mu)$ where $U = Q/(2\rho H^2)$ is the flow rate-based average velocity in the mixing channel, $H = 200\mu$m is height of the channel and $d = 267$ μm is hydraulic diameter.

For the quantitative characterization of the mixing efficiency the following parameter was used:

$M = 1 - \sqrt{\sigma/\sigma_0}$, where $\sigma = \frac{1}{V}\cdot\int_V \left(f - \bar{f}\right)^2 dV$ is the concentration of component f standard deviation from its mean value $\bar{f}$ by the volume (V) of mixer, $\sigma_0 = \bar{f}(1-\bar{f})$ is the maximum standard deviation.

Experimental Set Up

The diagram of experimental setup is shown in Fig. 1. Imaging system consisted of epifluorescence inverted microscope (Carl Zeiss AxioObserver.Z1) with lenses 20x/NA = 0.3 and 5x/NA = 0.12 (number 1 in Fig.1) for micro-PIV and micro-LIF experiments, respectively. Lighting and record the images on a digital camera using a measuring complex “POLIS” (number 3 in Fig. 1) were carried out. This complex included a double-pulsed Nd:YAG laser with 50 mJ energy, 532 nm wavelength and 8 Hz pulse repetition frequency, covering the flow through the lens of the microscope. To entering the light into the microscope the liquid light guide and the fibers interface unit to the optical path of the microscope were used. Lighting of the microchannel during the micro-LIF experiments was carried out using a mercury lamp. Crosscorrelation digital camera recorded the images with 2048×2048 pixels resolution, which are then transferred to a personal computer for processing. Synchronization of the system was carried out using a programmable processor. Controlling of the experiment and data processing were carried out using the software package ActualFlow.

Fluid motion control using infusion syringe pump (number 5 in Fig. 1) with adjustable liquid flow rate was carried out. The flow of liquid sow by fluorescent tracers from DukeScientific firm. The particles were composed of melamine resin, labeled with fluorescent dye Rhodamine B. The particle density is 1.05 g/cm^3, average diameter is 2 μm, the standard deviation is 0.04 μm. To register the light emitted from the particles, and the suppression the light reflected from the channel, beam-splitting cube, consisting of a dichroic mirror and two filters for excitation and detection of Rhodamine B was used.

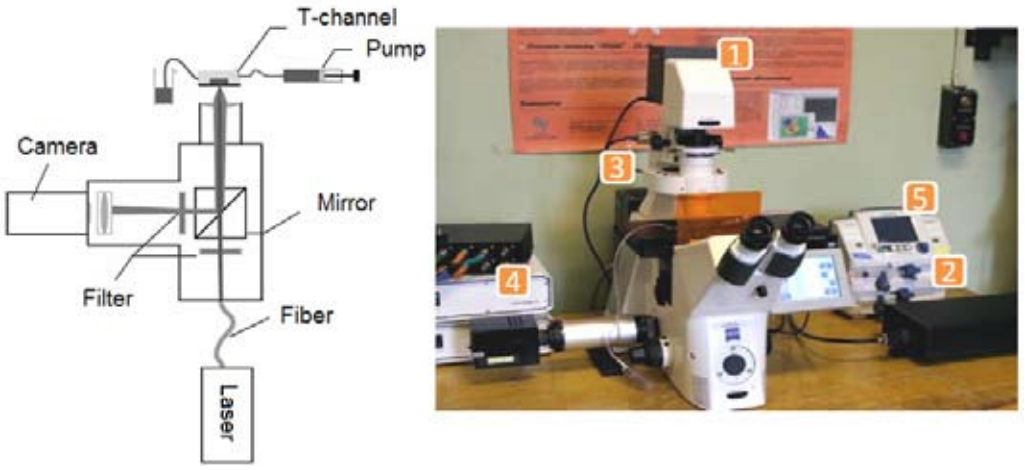

Fig. 1. The experimental setup

Micro-PIV and micro-LIF experiments were conducted at Reynolds numbers ranging from 10 to 300. The measurements were carried out in three regions of the T-mixer (so that the velocity field has been calculated up to seven calibers from the mixing channel entrance).

Concentration range in which the luminescence intensity of the fluorophore has a linear dependence on concentration was determined to calibrate the measurements. For this purpose, the T-channel is fed aqueous solutions of Rhodamine 6J in the following concentrations: 0 mg/l, 10 mg/l, 25 mg/l and 40 mg/l, 50 mg/l, 62.5 mg/l and 75 mg/l. For every concentration of the fluorophore the image of the channel was registered. As a result, linear dependence of the fluorophore radiation intensity was found at concentrations less than 62.5 mg/l. Thus, the relationship between the concentration of the fluorophore and the intensity of the image at each point of the channel was obtained.

Comparison of Calculations with Experimental Data

The Reynolds number in the range from 1 to 1000 was varied in the calculations. At low Reynolds numbers ($Re < 5$) in the mixer occurs steady irrotational flow. Mixing in this case occurs due to usual molecular diffusion and mixing efficiency is quite low [15] (see Fig. 2). Further, with increasing Reynolds number a pair of symmetrical horseshoe vortices (Dean vortices) formed in the mixer. They generated at the left end of the mixer wall (see Fig. 3, left) and extended into the channel on the mixing length, depending on the Reynolds number. Horseshoe vortices appear due to the development of secondary flows caused by the centrifugal force associated with rotation of the flow. Dean vortex structure is shown in Fig. 4 with isosurface $\lambda 2$. Here $\lambda 2$ is the second eigenvalue of the tensor ($\mathbf{SS} + \mathbf{\Omega\Omega}$), where $\mathbf{S}$ is the rate of strain tensor, and $\mathbf{\Omega}$ is the vorticity tensor.

The flow in this case is symmetric about the central longitudinal plane of the mixer. Each horseshoe vortex, being in the range of one liquid, does not cross the media mixing boundary, so the boundary between the media remains almost flat. This is clearly seen on the Fig. 3 (right). And because the diffusion Peclet number increased with increasing Reynolds number, the mixing efficiency decreased (see Fig. 2).

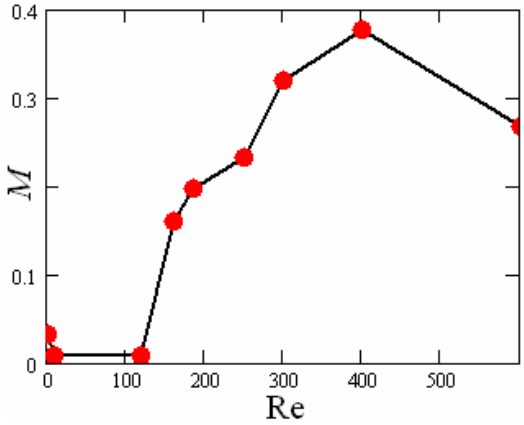

Fig. 2. Mixing efficiency versus Reynolds number

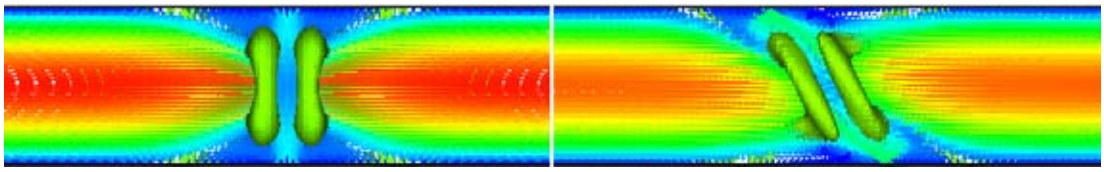

Fig. 3. Isolines of the velocity field in the cross section of the mixer (end view) and isosurface λ2. Re = 120 (left) and Re = 186 (right)

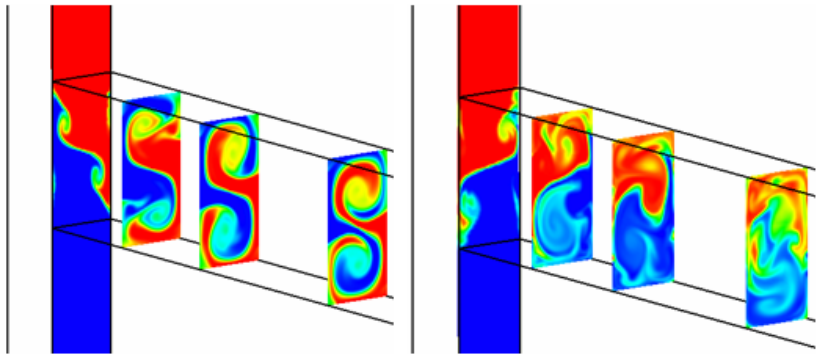

Fig. 4. Izolines of the dye concentrations in 4 longitudinal sections of the mixer: Re = 186 (left), Re = 600 (right)

When the Reynolds number reaches 150, the vortices lose their symmetry (see Fig. 3, right). They are rotated through an angle of 45° relative to the central plane of the mixer cross-section. S-shaped vortex formed. This is particularly clearly shown in Fig. 4 (left), where mixing is shown by isolines of the dye concentration in the four cross sections of the mixer. First left section is located at the entrance to the mixing channel, second – at the distance of 100 μm from the entrance, third – at the distance of 200 μm and fourth – at the distance of 400 μm. It is important to emphasize that flow is still stationary.

However, due to the fact that the intensity of the vortices in the asymmetric flow regime increases significantly, they extend through the mixing channel up to the exit. The presence of swirling flow in

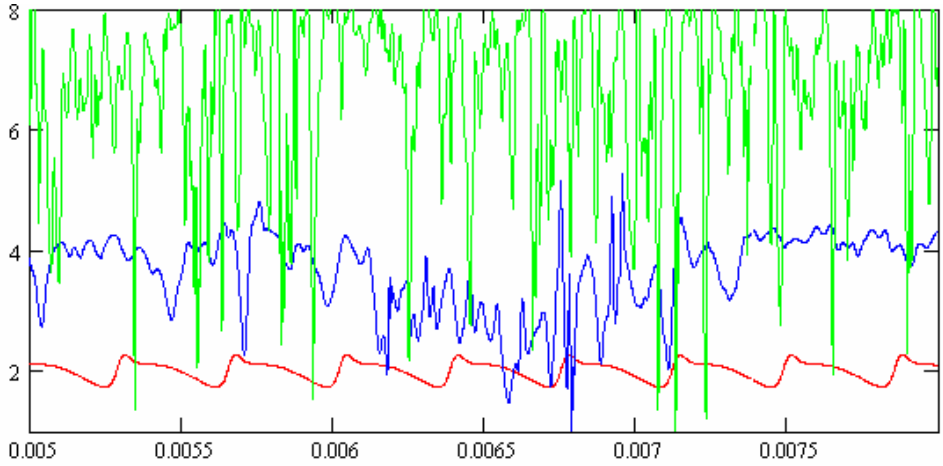

Fig. 5. The flow velocity versus time in point located at the mixer outlet. Red – Re = 300, blue – Re = 600, green – Re = 1000

the mixing channel leads to a layered structure of the miscible fluids formation. The contact surface of the miscible fluids in the layered structure is developed, which leads to a sharp increase of the mixing efficiency (see Fig. 2). In the transition from a symmetric flow regime (Re < 150) to the asymmetric (Re > 150), the mixing efficiency increases by 25 times.

Described stationary asymmetric flow regime is observed in the range of Reynolds numbers from 140 to 240. Starting from a Reynolds number of approximately equal 240, flow ceases to be stationary. In the range of Reynolds numbers 240 < Re < 400 implemented periodic flow regime. In particular, it means that the flow velocity is also a periodic function of time. In Fig. 5 this flow regime corresponds to the lower curve. The flux oscillation frequency f is determined by many factors: the geometry of the channel, the fluid viscosity, the Reynolds number. To describe this dependence, we introduce the Strouhal number $St = (fd^2)/(\nu Re)$, which is actually the dimensionless frequency of flow oscillations normalized by the Reynolds number (ν is the kinematic viscosity). A diagram of the Strouhal number versus Reynolds number is shown in Fig. 6 (squares). The oscillation frequency increases monotonically to a value of Re = 300 and then decreases slightly.

Our calculations data are correlated accurately with experimental one [16], which in Fig. 6 are marked with red tags. Maximum differences are observed at high Reynolds numbers, but it should be noted that the experimental data were obtained for a channel with cross-sectional dimensions of 600μm×300μm.

Meanwhile, the layered mixing structure which was formed at Re > 150 is preserved in whole, and due to transverse flow fluctuations in the unsteady flow regime the mixing efficiency increases to about M = 40% (see Fig. 2).

Starting from a Reynolds number of 450, the frequency of flow oscillations gradually decays. Firstly flow becomes quasiperiodic (450 < Re < 600), and then almost chaotic (Re > 600). The frequency spectrum of the velocity field becomes sufficiently filled, and is close to the continuous. This is clearly seen in Fig 5 (see also Fig. 4 (right)), where the Reynolds number 600 corresponds to the medium curve, and the Reynolds number 1000 corresponds the top one.

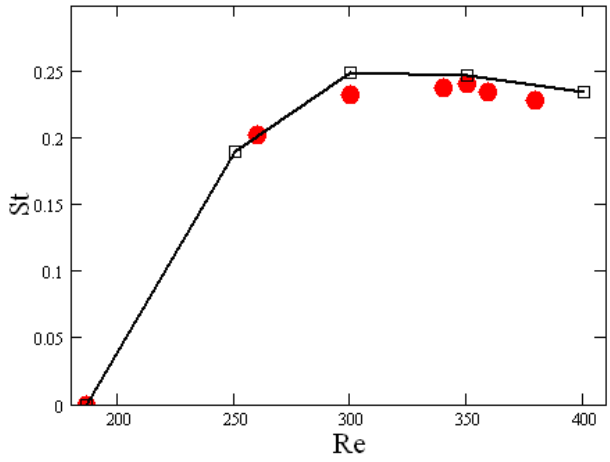

Fig. 6. Strouhal number versus Reynolds number

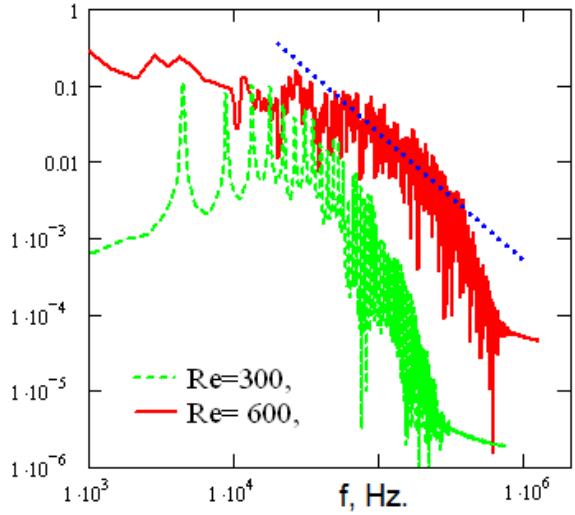

Fig. 7. The spectrum of the turbulent kinetic energy

The distribution of the flow pulsation kinetic energy ε by frequencies for Re = 600 is shown in Fig. 7. This spectrum is obtained for a point located in the center of the mixing channel at a distance of 400 μm from the entrance. Straight dashed line on the graph corresponds to the universal law of the Kolmogorov-Obukhov.

Although for Re = 600 the spectrum can not be considered complete continuous, as in the case of developed turbulent flow, nevertheless, there are a large number of frequencies and the inertial range, which suggests, at least availability of the transitional flow regime. Such early beginning of turbulence for channels flow occurs due to the development of Kelvin-Helmholtz instability at the entrance of the mixing channel.

However, calculations show that if mixing channel is long enough, then with increasing of the distance from the flow confluence the pulsations gradually damped, the flow became laminar and,

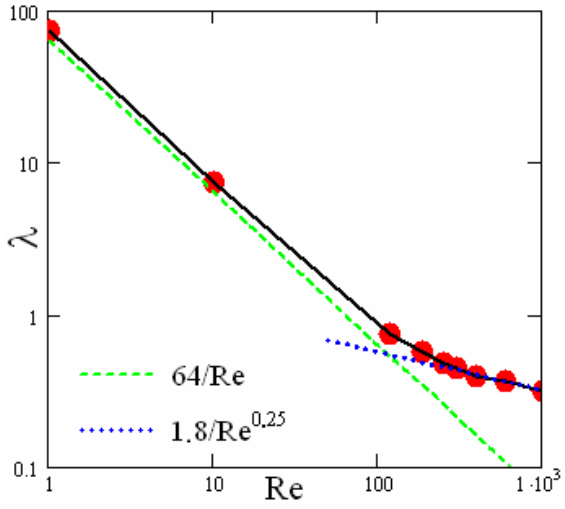

Fig. 8. Friction factor versus the Reynolds number

as expected, the steady velocity profile is formed. The length of the velocity profile establishment, of course, depends on the Reynolds number. To show it the problem for a channel 7000 μm length was solved. The obtained data is illustrated in Fig. 10, where compares the velocity profiles for the two Reynolds numbers: 30 and 120.

This coefficient is determined by formula $\lambda = (2\Delta P d)/(\rho U^2 L)$ where ΔP is the pressure drop in the channel, and L is the length of the channel. The dark mark and the line connecting them correspond to calculation. To compare the results the values of friction factor for steady laminar flow in a rectangular channel is shown on the graph by the dashed line.

For a channel with height-to-width ratio equal to 0.5 the friction factor is close to 64/Re. Nevertheless, the analysis shows that for small Reynolds numbers the friction factor in micromixer on average 20-30% higher than for steady flow. Then the friction factor dramatically deviate from the dependence $\lambda = 64/Re$, indicating the laminar-turbulent transition. The calculated data of the friction factor in micromixer at moderate Reynolds numbers is well described by the dependence $\lambda = 1.8/Re^{0.25}$. Obtained value of the friction factor is almost six times higher than the classical Blasius dependence ($\lambda = 0.316/Re^{0.25}$) for the developed turbulent flow in the direct channel. Such large difference is due to the presence of a turning flow at the channel inlet, and its vortex in the mixing channel. In particular, the pressure along the channel does not change monotonically. In the transition to turbulence, S-shaped vortex structure, that was formed in the mixing channel at $Re > 150$ and existed in the transient regime collapses. The flow is divided into a set of sufficiently large eddies. Because of it the contact area between the miscible liquids reduced. And so mixing efficiency slightly decreased on transition to turbulence (see Fig. 2). Naturally, with further increase of the Reynolds number a lot of small-scale vortices appeared in the flow.

As a consequence, the mixing efficiency in the developed turbulent flow far exceeds suitable value for laminar flow.

Comparison of the experimentally measured by micro-PIV and calculated velocity profiles in the central section of the mixing channel at 2.5 calibers from the input are shown in Fig. 9. The appearance

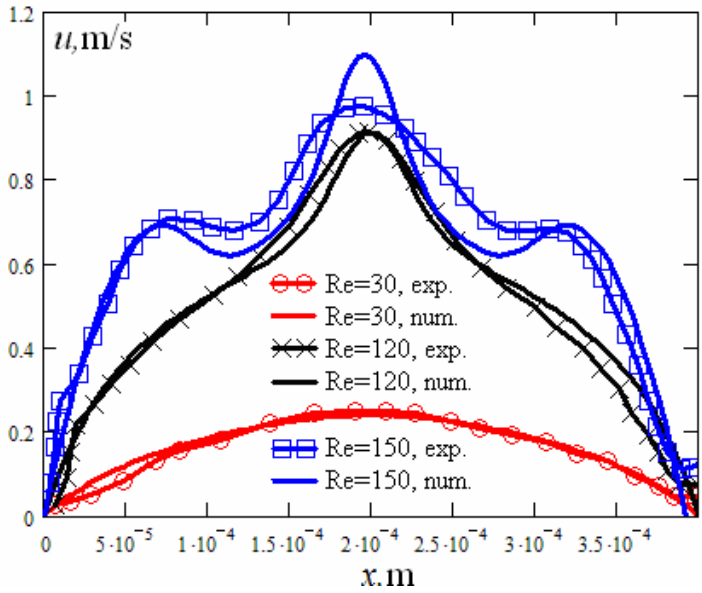

Fig. 9. Velocity profiles in the central cross section of the channel.

of curve bends in the velocity profiles associated with the occurrence of an S-shaped structure. Overall agreement between the experimental and calculated data is quite good, the maximum error does not exceed 10%, but with increasing Reynolds number it's increased. This is due to essentially three-dimensional structure of the flow at a given Reynolds number.

For example, in micro-PIV measured velocity field is the average depth of correlation (in this experiment it was equal to the depth of correlation 37 microns), the gradient of the longitudinal velocity of the channel depth has led to a smoothing of the velocity profile in the micromixer. A qualitative comparison of calculated and experimental velocity fields in the central longitudinal section of the mixer is shown in Fig. 10. Here also there is quite satisfactory agreement between the calculated and experimental data.

To compare the concentration fields obtained by numerical simulation and in the experiment the spatial averaging of the calculated data on the depth of the T-mixer was carried out. The concentration field in the 11 sections of XY plane on the depth of the T-mixer symmetrical about its center was taken to average.

Concentration field for each section averaged spatially using a "running average" filter with a round window the same diameter as the point spread function diameter in this section. The resulting concentration field was calculated as the arithmetical mean of 11 sections. The averaged concentration field obtained by numerical simulation and in the experiment for different Reynolds numbers are shown in Fig. 11 and Fig. 12. In whole, there is good qualitative agreement.

Conclusions

Thus, this modeling allows to sort out for the incompressible fluid flow in T-type micromixer following flow regimes:

- The steady vortex-free flow, realized at low Reynolds numbers (Re < 5).

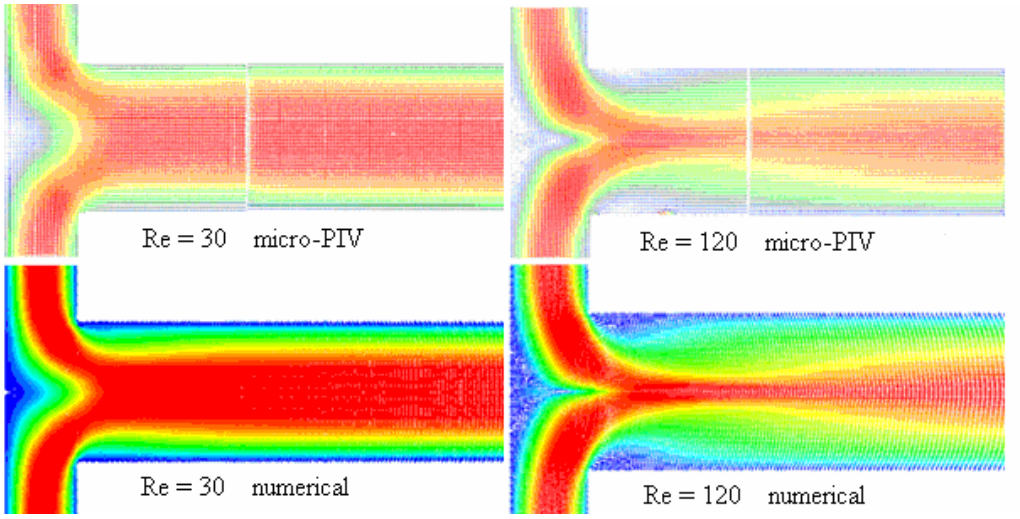

Fig. 10. Average experimental and calculated velocity field in the central section of micromixer for Reynolds numbers equals 30 and 120

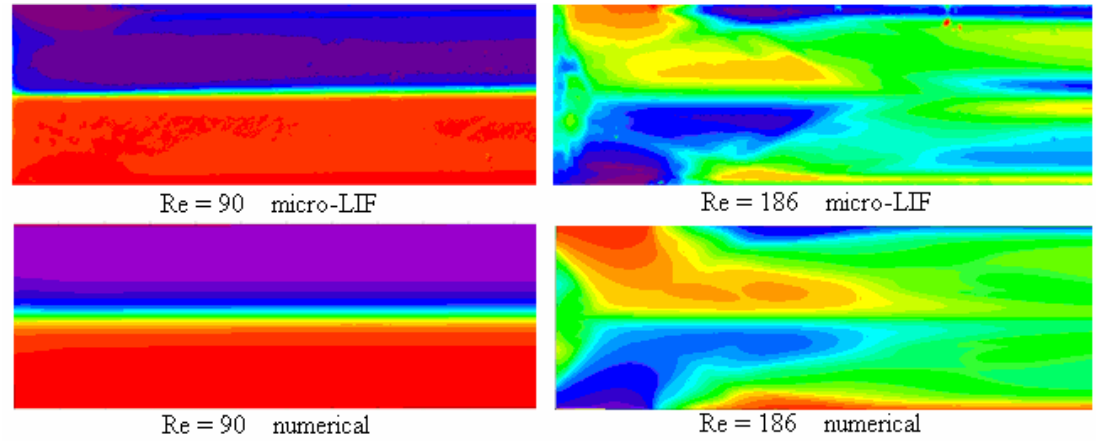

Fig. 11. Averaged concentration field in the central section of micromixer for Re=90 and Re=186

- The steady symmetric vortex flow with two symmetric horseshoe vortices at the mixing channel inlet. This regime realized when the Reynolds numbers vary in the range $5 < Re < 150$.
- Steady asymmetric vortex flow is observed in the range of Reynolds numbers $150 < Re < 240$. Formed at the entrance horseshoe vortices lose their symmetry and rotated at 45° relative to the central longitudinal plane of the mixing channel. S-shaped vortices formed.
- Unsteady periodic flow is realized in the range $240 < Re < 400$.
- Almost a stochastic flow regime ($400 < Re < 1000$). S-shaped vortex structures observed at lower Reynolds numbers collapsed.

The mixing efficiency increases dramatically during formation the S-shaped vortex structures in the flow and then continues to grow in an unsteady periodic regime. In paper [15] was shown that the mixing efficiency can be substantially increased by changing flow rate at the inlet of the

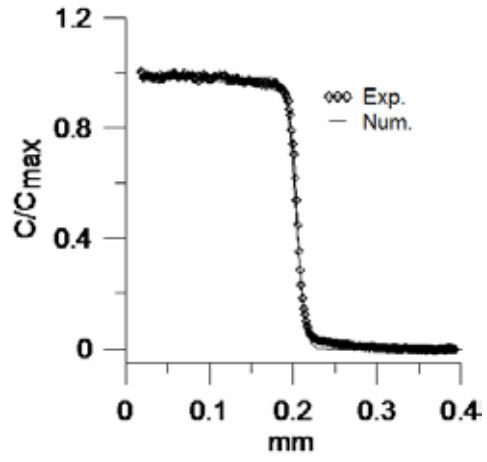

Fig. 12. The normalized concentration profiles across the mixing channel for Re = 30

mixer in a certain way by harmonical law. In fact, here we have some "autocontrol" of the mixing process.

Usually to ensure the efficient mixing, the mixer length should be large enough. Naturally, this leads to a significant loss of pressure caused by friction at the walls. On the other hand, such losses can be reduced by using hydrophobic or even ultrahydrophobic coats. In microflows the slip length can reach tens of microns. As it shown in [15], if the Reynolds numbers were low the mixing efficiency particularly didn't change. However, the situation is changing at moderate Reynolds numbers. The presence of wall slip leads to a significant change in flow regimes. If there are slip conditions the flows are rebuilt. Simulations show, for example, that at Reynolds numbers equals 200 and sufficiently large slip lengths the two-vortex structure mentioned above is transformed into one-vortex. Naturally, the mixing efficiency increased too. For this mixer an increase is about 30%. On the other hand, the pressure drop decreases monotonically with increasing the slip length (for investigated mixer for about 30-40%). Thus, using a hydrophobic coats (slip conditions) one can control the flow regimes.

Acknowledgment

This work was supported in part by the Russian Foundation for Basic Research (Grants №. 10-01-00074 and 11-08-01268) and the Federal Special Program "Scientific and scientific-pedagogical personnel of innovative Russia in 2009-2013" (№ 16.740.11.0642, 14.A18.21.0344, 14.132.21.1750, 8756).

References

[1] *Tabeling P.* Introduction to microfluidics, Oxford University Press, 2005.

[2] *Karnik R.* // Encyclopedia of microfluidics and nanofluidics, 2008. P. 1177–1186.

[3] *Vanka S.P., Luo G. and Winkler C.M.* // AIChE J. 50 (2004) 2359–2368.

[4] *Aubina J., Fletcherb D.F. and Xuereb C.* // Chem. Eng. Sci. 60 (2005) 2503–2516.

[5] *Hoffmann M., Schluter M., Rubiger N.* // Chemical Engineering Science 61 (2006) 2968–2976.

[6] *Mansur E.A., Mingxing Y.E., Yundong W., Youyuan D.* // Chinese J. Chemical Eng. 16(4) 2008. P. 503–516.

[7] *Engler M., Kockmann N., Kiefer T., Woias P.* // Chem. Eng. J. 101 (2004) 315–322.

[8] *Telib H., Manhart M., Iollo A.* // Phys. Fluids 16 (2004) 2717–2731.

[9] *Wong S.H., Ward M.C.L., Wharton C.W.* // Sens. & Act. B. 100 (2004) 359–379.

[10] *Gobert C., Schwert F., Manhart M.* // Proc. ASME Joint U.S.-European Fluids Eng. Summer Meeting, Miami, Paper no. FEDSM2006-98035, 2006. P. 1053-1062.

[11] *Rudyak V.Ya., Minakov A.V., Gavrilov A.A. and Dekterev A.A.* // Thermophysics & Aeromechanics 15 (2008) 33–345.

[12] *Gavrilov A.A., Minakov A.V., Dekterev A.A. and Rudyak V.Ya.* // Sib. Zh. Industr. Matem. 13 (2010). № 4. P. 3–14.

[13] *Podryabinkin E.V., Rudyak V.Ya.* // J. Engineering Thermophysics. 20 (2011), No. 3. P. 320–328.

[14] *Minakov A.V., Rudyak V.Ya., Gavrilov A.A., Dekterev A.A.* // Journal of Siberian Federal University. Mathematics & Physics 3(2010), No. 2. P. 146–156.

[15] *Rudyak V.Ya., Minakov A.V., Gavrilov A.A. and Dekterev A.A.* // Thermophysics & Aeromechanics 17 (2010) 565–576.

[16] *Dreher S., Kockmann N., Woias P.* // Heat Transfer Engineering 30 (2009) 91–100.

Micro-LIF и численное исследование смешения в микроканале

А.В. Минаков[а,б], А.А. Ягодницына[б], А.С. Лобасов[а,б], В.Я. Рудяк[б,в], А.В. Бильский[б]

[а] Сибирский федеральный университет, Россия 660074, Красноярск, ул. Киренского, 28

[б] Институт теплофизики СО РАН, Россия 630090, Новосибирск, пр. Лаврентьева, 1

[в] Новосибирский государственный архитектурно-строительный университет, Россия 630008, Новосибирск, ул. Ленинградская, 113

В статье с помощью численного моделирования и экспериментальных методов micro-PIV и micro-LIF исследованы режимы течения и смешения жидкостей в микромиксере Т-типа в широком диапазоне значений числа Рейнольдса от 1 до 1000. Поперечное сечение канала равнялось 200 мкм×400 мкм, а длина канала была равна 3000 мкм. Было обнаружено пять различных режимов течения: (I) стационарное безвихревое течение; (II) стационарное симметричное вихревое течение с двумя подковообразными вихрями; (III) стационарное асимметричное вихревое течение; (IV) нестационарное периодическое течение; (V) хаотическое течение. Максимальное значение эффективности смешения наблюдается при стационарном асимметричном вихревом течении. В этом случае в потоке формируются S-образные вихревые структуры. Показано хорошее соответствие расчётных и экспериментальных данных.

Ключевые слова: микротечение, микромиксеры, микроканалы, CFD, Micro-PIV, Micro-LIF.